A Negative Single-Input/Multi-Output LED Driver and Its Analysis Method

Kei Eguchi and Kanji Abe
Department of Information Electronics, Fukuoka Institute of Technology, 3-30-1 Wajiro-higashi, Higashi-ku, Fukuoka, Japan
Email: eguti@fit.ac.jp, mam15001@bene.fit.ac.jp

Sawai Pongswatd
Department of Instrumentation and Control Engineering, King Mongkut's Institute of Technology Ladkrabang, Ladkrabang, Bangkok, 10520 Thailand
Email: klsawai@kmitl.ac.th

Shinya Terada and Ichirou Oota
Department of Information, Communication and Electronic Engineering, National Institute of Technology, Kumamoto College, 2659-2 Suya, Koushi, Kumamoto, 861-1102 Japan
Email: {terada, oota-i}@kumamoto-nct.ac.jp

***Abstract*—A negative single-input/multi-output (SIMO) LED driver is proposed in this paper. Unlike the conventional LED driver using SIMO boost converters, the proposed LED driver using an SIMO buck-boost converter offers a negative stepped-down voltage to drive LED's cathodes. By turning on output switches in rotation during a transferring process, the proposed driver can suppress the imbalance among output currents. This paper also presents a novel analysis method to estimate properties of the SIMO LED driver using a buck-boost converter. By assuming a five-terminal equivalent circuit, the proposed analysis method can derive the power efficiency and output voltages without complex matrix calculations. The theoretical analysis and experiments show the effectiveness of the proposed SIMO LED driver.**

***Index Terms*—DC-DC converters, buck-boost converters, switching converters, negative outputs, white LEDs, back-lighting applications**

I. INTRODUCTION

As one of the most ideal backlight solutions, a light-emitting diodes (LEDs) backlighting has been used in electronic appliances. To drive LEDs, several types of switching converter topologies have been proposed [1]-[12]. These converter topologies can be divided into two types: capacitor-based converter topology and inductor-based converter topology.

In the capacitor-based LED driver, a single-input/single-output (SISO) charge-pump has been commonly used [1], [2], where a positive stepped-up voltage is generated to drive the LED's anodes. The charge-pump can realize no flux of magnetic induction, small volume, and light-weight, because no magnetic component is required. However, when the LEDs are mismatched, the charge-pump must switch to step-up mode due to the bad forward voltage of only one LED. To overcome this problem, Kim suggested the SISO LED driver using a negative charge-pump [3]. By employing the individual mode switching, the negative charge-pump achieves high power efficiency. However, it is difficult to improve power efficiency further, because the conversion ratio of capacitor-based converters is predetermined by circuit structure. For this reason, energy loss caused by linear current regulation is considerably large.

On the other hand, an SISO boost converter has been widely used [4], [5] in the inductor-based LED driver. Unlike the capacitor-based LED drivers [1]-[3], the output voltage of the inductor-based LED driver can be adjusted by controlling the duty cycle of clock pulses. Therefore, the inductor-based LED driver achieves higher efficiency than capacitor-based LED drivers. Following this study, the LED drivers using an SISO buck-boost converter have been proposed [6]-[9] to regulate the LED currents supplied with a wide-range input voltage source. As in the case of the negative charge-pump, the LED driver using a buck-boost converter drives the LED's cathodes. However, the circuit size of the inductor-based LED driver is larger than that of the capacitor-based LED driver, because the inductor-based LED driver requires magnetic components.

For this reason, in order to reduce the number of magnetic components, a single-input/multiple-output (SIDO) switching converter [10]-[12] has been proposed in recent years. Fig. 1 illustrates the block diagram of the LED driver using a positive SIMO converter. In the conventional driver shown in Fig. 1, a positive stepped-up voltage is provided to drive the LEDs' anodes. For example, He et al. suggested the SIMO LED driver using a flyback converter [10]. However, the conventional

Manuscript received May 18, 2015; revised August 6, 2015.

doi: 10.18178/ijoee.3.3.179-185

driver reported in [10] is bulky, because the driver reported in [10] requires a transformer. As distinct from the LED driver using a transformer, Hong *et al.* proposed the SIMO LED driver using a boost converter [11]. By using a non-isolated converter, the conventional driver reported in [11] can achieve smaller size than the driver reported in [10]. However, as described in [12], the power efficiency of the LED driver reported in [11] decreases significantly due to a linear current regulation element for each channel. To overcome this problem, Kim *et al.* suggested the SIMO LED driver using a boost converter with a time-division multiplexing conduction scheme. By turning on output switches by N+1 (=2, 3, …)-phase clock pulses, the LED driver reported in [12] can eliminate linear current regulation elements.

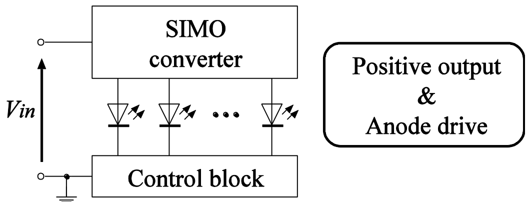

Figure 1. Block diagram of the LED driver using a positive SIMO converter.

In this paper, we propose a negative SIMO LED driver. Unlike the conventional SIMO LED drivers, the proposed LED driver employs a buck-boost converter to drive LED's cathodes, because the LED driver using an SISO buck-boost converter can achieve not only a wider input range but also better performance than the LED driver using a SISO boost converter as described in [9]. Furthermore, by turning on output switches in rotation during a transferring process, the proposed driver can suppress the imbalance among output currents.

This paper also presents a novel analysis method to estimate properties of the SIMO LED driver using a buck-boost converter. In the traditional theoretical analysis of a switching DC-DC converter with magnetic elements, the state-space averaging method has been commonly used [13]-[15]. However, the state-space averaging method requires complex matrix calculations. By assuming a five-terminal equivalent circuit, the proposed method derives the power efficiency and output voltages without complex matrix calculations. To confirm the validity of the proposed converter, theoretical analysis and experiments are performed.

The rest of this paper is organized as follows. In Section 2, the circuit configuration of the proposed driver is presented. In Section 3, the property of the proposed driver is analyzed by the proposed analysis method. Experimental results are shown in Section 4. Finally, conclusion and future work are drawn in Section 5.

II. Circuit Configuration

Fig. 2 illustrates the circuit configuration of the proposed SIMO LED driver with N (=2, 3, 4, …) outputs. Unlike the conventional SIMO LED drivers [9]-[11], a buck-boost converter is employed in the proposed SIMO LED driver. The basic operation of the proposed driver is as follows. When the transistor switch S_0 turns on, the inductor L is charged by the input voltage V_{in}. Next, the output switches S_1, S_2, …, S_N are turned on in rotation. In State-T_1 - T_N, the LED's cathodes are driven by a negative stepped-down voltage, where the turn-on sequence of S_1, S_2, …, S_N is permutated. Unlike the conventional control method described in [12], the switches S_1, S_2, …, S_N of the proposed driver are turned on in rotation by N-phase clock pulses. (See in Fig. 2.)

To help readers' understanding, let us discuss the simplest example of the proposed driver shown in Fig. 3. In Fig. 3, State-T_0 is the charging process of the inductor L and States-T_1 and T_2 are the transferring process. In the transferring process, the turn-on sequence of S_1 and S_2 is permutated to suppress the imbalance among LED currents. (See in Fig. 3.) Therefore, the output voltages are expressed as if the duty cycle D is set to T_0/T and the proposed driver operates in a continuous conduction mode (CCM).

$$V_{out1} \cong V_{out2} \cong V_{in} + \left(\frac{D}{1-D}\right)V_{in}$$

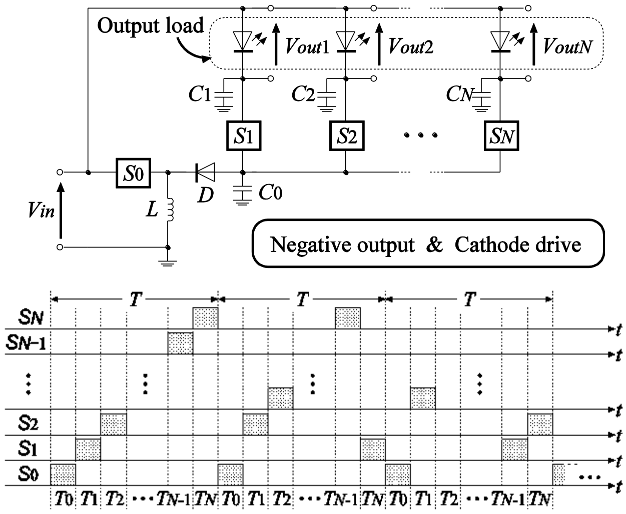

Figure 2. Proposed LED driver using a single-input multiple-output buck-boost converter.

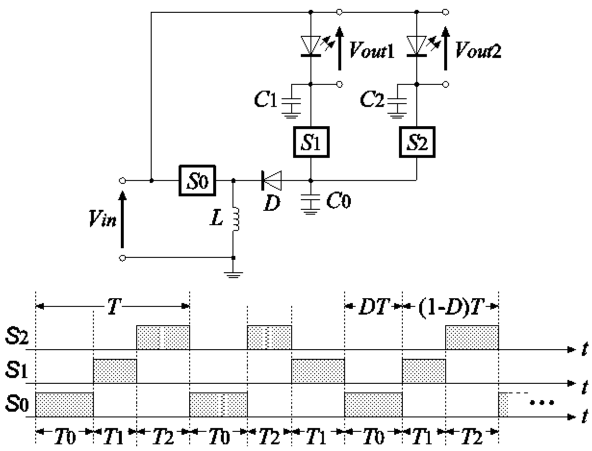

Figure 3. Proposed LED driver with two outputs.

The detailed theoretical analysis concerning the proposed driver will be described in the following section.

III. Theoretical Analysis

A. Proposed LED Driver

To analyze steady-state behavior of the proposed driver, theoretical analysis is performed concerning the proposed driver with two outputs. By assuming a five-terminal equivalent circuit illustrated in Fig. 4, the proposed analysis is performed, because it is known that the general equivalent circuit of the single-input single-output SC DC-DC converter can be expressed by a four-terminal circuit [16], [17]. In Fig. 4, m is the ratio of an ideal transformer, R_{ac} is the resistance to express the ripple loss of a reactor, R_{o12}, R_{o1}, and R_{o2} are output resistances, and R_{L1} are R_{L2} output loads. Unlike the state-space averaging method [13]-[15], the proposed analysis method derives these parameters from instantaneous equivalent circuits without complex matrix calculations. To save space, the theoretical analysis will be discussed concerning the proposed driver operating in CCM.

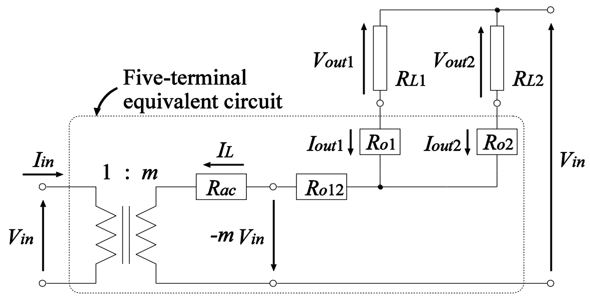

Figure 4. Proposed five-terminal equivalent model.

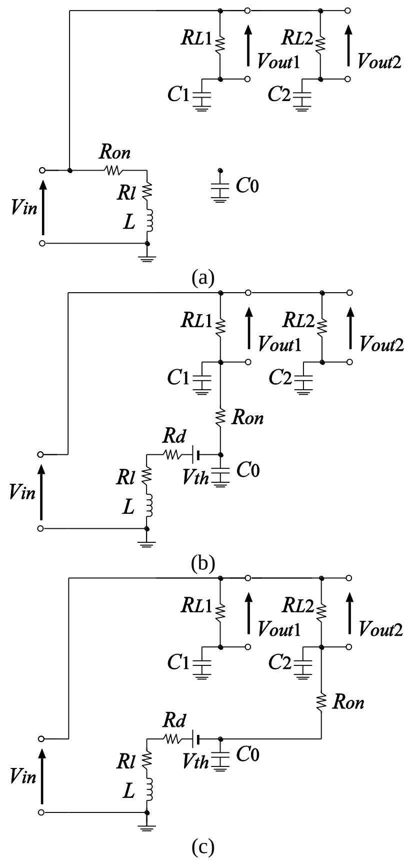

Figure 5. Instantaneous equivalent circuits of the proposed driver: (a) State-T_0, (b) State-T_1, and (c) State-T_2.

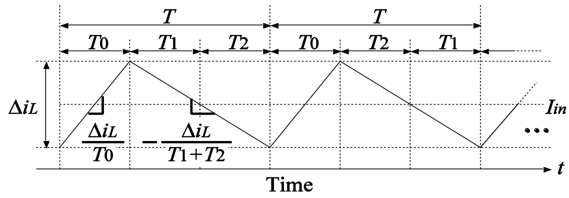

Figure 6. Inductor current.

Fig. 5 illustrates the instantaneous equivalent circuits of the proposed driver with two outputs, where R_{on} is the on-resistance of the transistor switch, R_d is the on-resistance of the diode switch, R_l is the resistance of the inductor, L is the ideal inductor, and V_{th} is the threshold voltage of the diode switch. When the proposed driver operates in CCM, the current through the inductor L is expressed as shown in Fig. 6. In Fig. 6, the inductor currents in State-T_0, T_1 and T_2 are expressed as:

$$i_{L,T_0}(t)=\left(\frac{\Delta i_L}{T_0}\right)t+\left(I_{in}-\frac{\Delta i_L}{2}\right) \tag{1}$$

$$i_{L,T_1}(t)=-\left(\frac{\Delta i_L}{T_1+T_2}\right)t+\left\{I_{in}+\frac{1+D}{2(1-D)}\Delta i_L\right\} \tag{2}$$

And:

$$i_{L,T_2}(t)=-\left(\frac{\Delta i_L}{T_1+T_2}\right)t+\left\{I_{in}+\frac{1+D}{2(1-D)}\Delta i_L\right\} \tag{3}$$

where:

$$T_0=DT \tag{4}$$

$$T_1+T_2=(1-D)T \tag{5}$$

And:

$$T=\sum_{i=0}^{2}T_i \tag{6}$$

In (1)-(3), Δi_L is the variation of the inductor current (see Fig. 6). Using (1) - (3), the variation of the inductor current in State-T_0 is given by:

$$\begin{aligned}\Delta i_L &= i_{L,T_0}(T_0)-i_{L,T_0}(0)\\ &=\frac{1}{L}\int_0^{T_0}V_{in}dt\\ &=\frac{V_{in}}{L}T_0\end{aligned} \tag{7}$$

On the other hand, the variation of the inductor current in State-T_1 and T_2 is given by:

$$\begin{aligned}-\Delta i_L &= i_{L,T_2}(T)-i_{L,T_1}(T_0)\\ &=\frac{1}{L}\int_{T_0}^{T}V_L dt\\ &=\frac{V_L}{L}(T_1+T_2)\end{aligned} \tag{8}$$

where V_L denotes the voltage of the inductor. From (7) and (8), we have the following relations:

$$V_L=-\left(\frac{D}{1-D}\right)V_{in}\ \text{and}\ I_L=-\left(\frac{1-D}{D}\right)I_{in} \tag{9}$$

where I_L is the average inductor current and I_{in} is the average input current. From (9), the parameter m in Fig. 4 is obtained as:

$$m = -\left(\frac{D}{1-D}\right) \tag{10}$$

Next, in order to derive the output resistances R_{o12}, R_{o1}, and R_{o2}, the consumed energy in one period is discussed. From Fig. 5, the consumed energy W_T can be expressed as:

$$W_T = \sum_{i=0}^{2} W_{Ti} \tag{11}$$

where:

$$W_{T_0} = \int_0^{T_0} \left(R_{on} + R_l\right)\left(i_{L,T_0}(t)\right)^2 dt \tag{12}$$

$$W_{T_1} = \int_{T_0}^{T_0+T_1} \left(R_l + R_d + R_{on}\right)\left(i_{L,T_1}(t)\right)^2 dt \tag{13}$$

And:

$$W_{T_2} = \int_{T_0+T_1}^{T} \left(R_l + R_d + R_{on}\right)\left(i_{L,T_2}(t)\right)^2 dt \tag{14}$$

Therefore, using (1)-(6), (12), (13), and (14), the total consumed energy in one period is obtained as:

$$\begin{aligned} W_T &= m^2\left\{R_{on} + R_l + (1-D)R_d\right\}T\left(I_{out1}\right)^2 \\ &+ m^2\left\{R_{on} + R_l + (1-D)R_d\right\}T\left(I_{out2}\right)^2 \\ &+ 2m^2\left\{R_{on} + R_l + (1-D)R_d\right\}T\left(I_{out1}\cdot I_{out2}\right) \\ &+ \frac{1}{12}\left\{R_{on} + R_l + (1-D)R_d\right\}T\left(\Delta i_L\right)^2 \end{aligned} \tag{15}$$

From Fig. 4, the consumed energy of the five-terminal equivalent model can be defined as:

$$\begin{aligned} W_T &:= \left(R_{ac} + R_{o12}\right)\left(I_L\right)^2 T \\ &+ \left(R_{o1}\right)\left(I_{out1}\right)^2 T + \left(R_{o2}\right)\left(I_{out2}\right)^2 T \\ &= \left(R_{o12} + R_{o1}\right)\left(I_{out1}\right)^2 T + \left(R_{o12} + R_{o2}\right)\left(I_{out2}\right)^2 T \\ &+ \left(2R_{o12}\right)\left(I_{out1}\cdot I_{out2}\right)T + R_{ac}\frac{(1-m)^2 L^2 \left(\Delta i_L\right)^2}{(DT)^2 Z^2}T \end{aligned} \tag{16}$$

where:

$$Z = R_{ac} + \frac{\left(R_{o1} + R_{L1}\right)\left(R_{o2} + R_{L2}\right)}{R_{o1} + R_{L1} + R_{o2} + R_{L2}} \tag{17}$$

Therefore, from (15) and (16), we have the resistances R_{o12}, R_{o1}, R_{o2}, and R_{ac} as follows:

$$R_{o1} = R_{o2} = 0 \tag{18}$$

$$R_{o12} = \left(\frac{D}{1-D}\right)^2\left\{R_{on} + R_l + (1-D)R_d\right\} \tag{19}$$

And:

$$R_{ac} = \frac{(1-D)^2 (DT)^2 \left(Z^{'}\right)^2}{12L^2}\left\{R_{on} + R_l + (1-D)R_d\right\} \tag{20}$$

where:

$$Z^{'} = R_{ac} + \frac{R_{L1}R_{L2}}{R_{L1} + R_{L2}} \tag{21}$$

Using (10), (18), (19), (20), and (21), the equivalent circuit of the proposed driver can be expressed by Fig. 7. The value of R_o in Fig. 7 completely is equal to the value R_o derived by using the state-space averaging method. In the CCM, R_{ac} becomes much smaller than R_o.

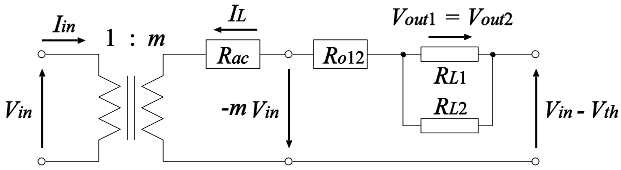

Figure 7. Equivalent circuit of the proposed driver.

From Fig. 7, the power efficiency and the output voltage of the proposed driver can be derived as:

$$V_{out1} = V_{out2} = \frac{R_{L1}R_{L2}}{R_{o12}\left(R_{L1} + R_{L2}\right) + R_{L1}R_{L2}}(1-m)V_{in} \tag{22}$$

And:

$$\eta = \frac{R_{L1}\left(I_{out1}\right)^2 + R_{L2}\left(I_{out2}\right)^2}{\left(R_{ac} + R_{o12}\right)\left(I_L\right)^2 + R_{L1}\left(I_{out1}\right)^2 + R_{L2}\left(I_{out2}\right)^2} \tag{23}$$

Equations (22) and (23) can be rewritten as:

$$V_{out1} = V_{out2} = \left(\frac{R_L}{2R_{o12} + R_L}\right)(1-m)V_{in} \tag{24}$$

And:

$$\eta = \frac{R_L}{2\left(R_{ac} + R_{o12}\right) + R_L} \tag{25}$$

If the output loads satisfy R_{L1}=R_{L2}=R_L. As (22)-(25) show, the proposed analysis method can estimate the characteristics without complex matrix calculations.

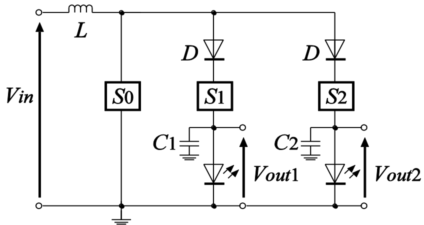

Figure 8. Conventional driver with two outputs.

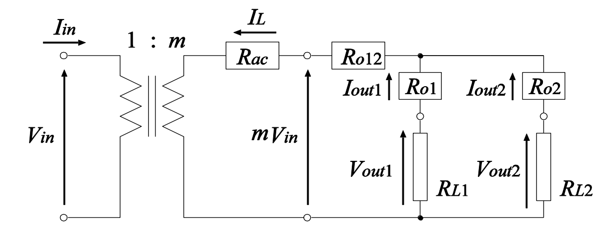

Figure 9. Five-terminal equivalent model for the conventional driver with two outputs.

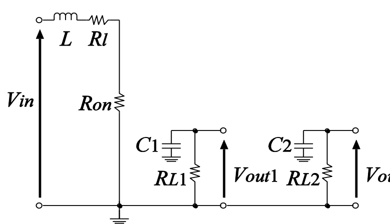

(a)

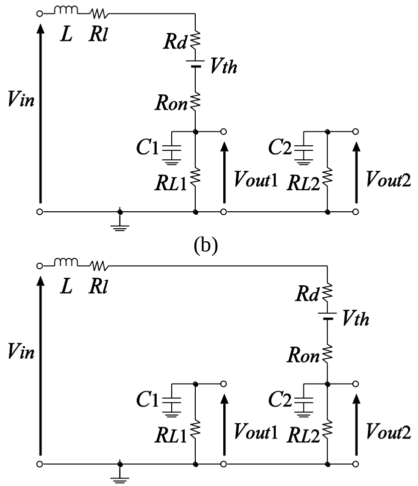

Figure 10. Instantaneous equivalent circuits of the conventional driver: (a) State-T_0, (b) State-T_1, and (c) State-T_2.

B. *Conventional LED Driver*

Fig. 8 illustrates the conventional LED driver using a boost converter with two outputs. The steady-state behavior of the conventional driver is analyzed by assuming a five-terminal equivalent circuit shown in Fig. 9. The instantaneous equivalent circuits of the conventional driver are expressed as Fig. 10, where the proposed control method is used to compare the characteristics of the conventional driver with that of the proposed driver. In Fig. 10, the current through the inductor L is also expressed as shown in Fig. 6. Therefore, the inductor currents in State-T_0, T_1 and T_2 are expressed as (1), (2), and (3), respectively. In Fig. 8, the variation of the inductor current in State-T_0 is given by:

$$\Delta i_L = i_{L,T_0}(T_0) - i_{L,T_0}(0) = \frac{1}{L}\int_0^{T_0} V_{in}\,dt = \frac{V_{in}}{L}T_0 \tag{26}$$

On the other hand, the variation of the inductor current in State-T_1 and T_2 is given by:

$$-\Delta i_L = i_{L,T_2}(T) - i_{L,T_1}(T_0) = \frac{1}{L}\int_{T_0}^{T}(V_{in}-V_L)dt = \frac{V_{in}-V_L}{L}(T_1+T_2) \tag{27}$$

From (26) and (27), we have the following relations:

$$V_L = \left(\frac{1}{1-D}\right)V_{in} \text{ and } I_L = (1-D)I_{in} \tag{28}$$

Therefore, the parameter m in Fig. 9 is obtained as:

$$m = \frac{1}{1-D} \tag{29}$$

As in the same way, the total consumed energy of the conventional driver is expressed as (15). On the other hand, the consumed energy of Fig. 9 can be defined as:

$$W_T := (R_{o12}+R_{o1})(I_{out1})^2 T + (R_{o12}+R_{o2})(I_{out2})^2 T + (2R_{o12})(I_{out1}\cdot I_{out2})T + R_{ac}\frac{m^2L^2(\Delta i_L)^2}{(DT)^2 Z^2}T \tag{30}$$

where:

$$Z = R_{ac} + \frac{(R_{o1}+R_{L1})(R_{o2}+R_{L2})}{R_{o1}+R_{L1}+R_{o2}+R_{L2}} \tag{31}$$

Therefore, from (15) and (30), we have the resistances R_{o12}, R_{o1}, R_{o2}, and R_{ac} as follows:

$$R_{o1} = R_{o2} = 0 \tag{32}$$

$$R_{o12} = \left(\frac{1}{1-D}\right)^2\{R_{on}+R_l+(1-D)R_d\} \tag{33}$$

And:

$$R_{ac} = \frac{(1-D)^2(DT)^2(Z')^2}{12L^2}\{R_{on}+R_l+(1-D)R_d\} \tag{34}$$

where:

$$Z' = R_{ac} + \frac{R_{L1}R_{L2}}{R_{L1}+R_{L2}} \tag{35}$$

As (19) and (33) show, the output resistance of the proposed driver, R_{o12}, is smaller than that of the conventional driver, because $0<D<1$. Therefore, from (23) and (25), the proposed driver can achieve higher efficiency than the conventional driver.

IV. Experiment

In the experiments, we focused on the verification of the circuit topology. Therefore, the experimental circuit was built with commercially available ICs on a bread board. Concretely, the experimental circuit of the proposed converter with two outputs was built with photo-MOS relay AQV212, Darlington sink driver TD62004 APG, microcontroller PIC12F1822, and diode 1N4007 on a bread board, where V_{in} = 3V, C_{out1} = C_{out2} = 10μF, L=10mH, T=600Hz and R_{L1}=R_{L2}=3kΩ.

Fig. 11 shows the measured clock pulses, where Fig. 11(a) describes the traditional control method and Fig. 11(b) describes the proposed control method. As Fig. 11(b) shows, the switches S_1 and S_2 is turned on in rotation.

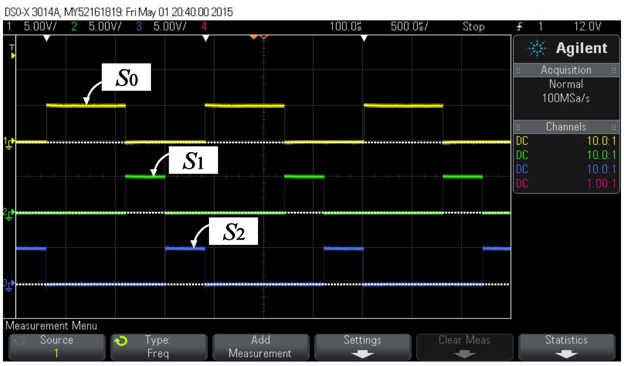

(a)

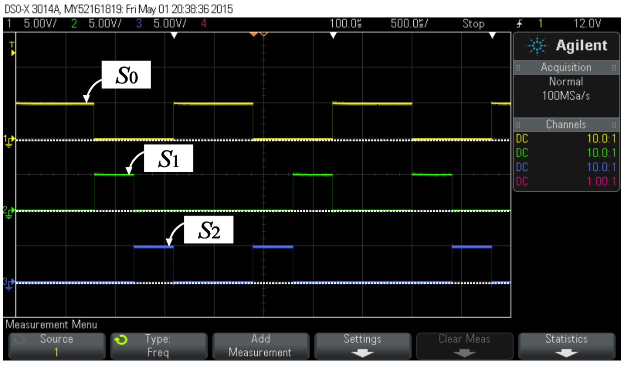

(b)

Figure 11. Measured clock pulses: (a) traditional control method and (b) proposed control method.

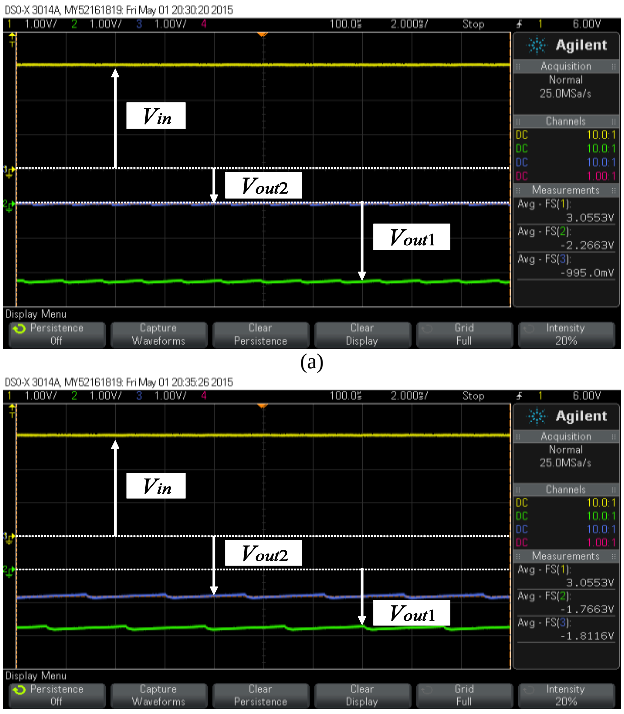

(a)

(b)

Figure 12. Measured output voltages: (a) traditional control method and (b) proposed control method.

Fig. 12 shows the measured output voltages. In the traditional control method of Fig. 12(a), the output voltages V_{out1} and V_{out2} are -2.27V and -1.00V, respectively. On the other hand, in the proposed control method, the output voltages V_{out1} and V_{out2} are -1.77V and -1.81V, respectively. As Fig. 12 shows, the proposed driver can reduce the current balance error. Concretely, in the conventional driver, the difference between the output currents I_{out1} and I_{out2} is 0.42mA. On the other hand, in the proposed driver, the difference between the output currents I_{out1} and I_{out2} is 15.1μA. In this case, the current balance error of the proposed driver is 0.47%.

V. Conclusion

A single-input/multi-output (SIMO) LED driver and its analysis method have been proposed in this paper. The results of this study are as follows: 1) By assuming a five-terminal equivalent circuit, the output voltages and power efficiency of the proposed SIMO LED driver were obtained without complex matrix calculations. The derived theoretical formulas will be helpful to estimate the characteristics of the proposed SIMO LED driver. Furthermore, theoretical results demonstrated that the proposed driver can achieve higher efficiency than the conventional driver; and 2) By turning on output switches in rotation, the imbalance among output currents was suppressed. In the proposed driver with two outputs, the current balance error of the proposed converter was 0.47%.

The detailed experiment of the proposed converter is left to a future study.

References

[1] R. Guo, Z. Liang, and A. Q. Huang, "A high efficiency transformerless step-up DC-DC converter with high voltage gain for LED backlighting applications," in *Proc. Twenty-Sixth Annual IEEE Applied Power Electronics Conference and Exposition*, 2011, pp. 6-11.

[2] Y. M. Wang, W. L. Deng, X. Y. Ma, W. Y. Huang, and J. K. Huang, "Design of a white LED backlight driver IC based on a new three-mode charge pump," in *Proc. IET Int. Conf. on Information Science and Control Engineering*, 2012, pp. 1-4.

[3] J. Kim, "Negative charge pumps achieve inductor-like efficiency for WLED backlights," *MAXIM Engineering Journal*, vol. 64, pp. 13-15, Jan. 2009.

[4] Y. T. Hsieh, B. D. Liu, J. F. Wu, C. L. Fang, H. H. Tsai, and Y. Z. Juang, "A high efficiency boost white LED driver for portable electronics applications," in *Proc. International Symposium on Next-Generation Electronics*, 2010, pp. 13-16.

[5] R. L. Lin, S. Y. Liu, and H. W. Chiang, "Optimal LED array combination for single-loop CCM boost driver," in *Proc. IEEE Industry Applications Conference*, 2012, pp. 1-7.

[6] K. Eguchi, S. Pongswatd, T. Watanabe, P. Pannil, K. Tirasesth, and H. Sasaki, "A white LED driver using a buck-boost converter," *IEEJ Transactions on Electrical and Electronic Engineering*, vol. 5, no. 5, pp. 613-614, Aug. 2010.

[7] K. Eguchi, S. Pongswatd, A. Julsereewong, I. Oota, S. Terada, and H. Sasaki, "Design of a dual-input buck-boost converter for mobile back-lighting applications," *International Journal of Innovative Computing, Information and Control*, vol. 8, no. 4, pp. 2901-2914, Apr. 2012.

[8] R. L. Lin, Y. C. Chang, and C. C. Lee, "Optimal design of LED array for single-loop CCM buck-boost LED driver," *IEEE Trans. on Industry Applications*, vol. 49, no. 2, pp. 761-768, Mar./Apr. 2013.

[9] R. L. Lin, J. Y. Tsai, S. Y. Liu, and H. W. Chiang, "Optimal design of LED array combinations for CCM single-loop control LED drivers," *IEEE Journal of Emerging and Selected Topics in Power Electronics*, vol. 3, no. 3, pp. 609-616, Mar. 2015.

[10] Y. He, J. Xu, and S. Zhong, "HB-LED driver based on single-inductor-dual-output switching converters in pseudo-continuous conduction mode," in *Proc. International Conference on Communications, Circuits and Systems*, 2013, pp. 15-17.

[11] S. I. Hong, J. W. Han, D. H. Kim, and O. K. Kwon, "A double-loop control LED backlight driver IC for medium-sized LCDs," in *Proc. IEEE International Solid-State Circuits Conference Digest of Technical Papers*, 2010, pp. 116-117.

[12] H. C. Kim, C. S. Yoon, D. K. Jeong, and J. Kim, "A single-inductor, multiple-channel current-balancing LED driver for display backlight applications," in *Proc. IEEE Energy Conversion Congress and Exposition*, 2013, pp. 15-19.

[13] A. Emadi and A. Abur, "Real time state estimation of multi-converter DC power electronic systems using generalized state space averaging method," in *Proc. IEEE 33rd Annual Power Electronics Specialists Conference*, 2002, pp. 881-886.

[14] M. M. Jalla, A. Emadi, G. A. Williamson, and B. Fahimi, "Real time state estimation of multi-converter more electric ship power systems using the generalized state space averaging method," in *Proc. 30th Annual Conference of IEEE Industrial Electronics Society*, 2004, pp. 1514-1519.

[15] S. Yang, K. Goto, Y. Imamura, and M. Shoyama, "Dynamic characteristics model of bi-directional DC-DC converter using state-space averaging method," in *Proc. IEEE 34th International Telecommunications Energy Conference*, 2012, pp. 1-5.
[16] K. Eguchi, S. Pongswatd, K. Tirasesth, H. Sasaki, and T. Inoue, "Optimal design of a single-input parallel DC-DC converter designed by switched capacitor techniques," *International Journal of Innovative Computing, Information and Control*, vol. 6, no. 1 (A), pp. 215-227, Jan. 2010.
[17] K. Eguchi, I. Oota, S. Pongswatd, A. Julsereewong, K. Tirasesth, and H. Sasaki, "Synthesis and analysis of a dual-input parallel DC-DC converter designed by using switched capacitor techniques," *International Journal of Innovative Computing, Information and Control*, vol. 7, no. 4, pp. 1675-1688, Apr. 2011.

Kei Eguchi was born in Saga, Japan in 1972. He received the B.Eng., the M.Eng., and the D.Eng. degree from Kumamoto University, Kumamoto, Japan in 1994, 1996, and 1999, respectively. His research interests include nonlinear dynamical systems, intelligent circuits and systems, and low-voltage analog integrated circuits.

From 1999 to 2006, he was an Associate Professor and a Lecturer in Kumamoto National College of Technology. From 2006 to 2012, he was an Associate Professor in Shizuoka University. In 2012, he joined the faculty of Fukuoka Institute of Technology, where he is now a Professor. Prof. Dr. Eguchi received ICIAE2015 Best Presentation Award, ICPEE2014 Excellent Oral Presentation Award, iCABSE2014 Excellent Paper Award, KKU-IENC2014 Outstanding Paper Award, ICEEN2014 Excellent Paper Award, JTL-AEME2013 Best Paper Award, ICTEEP2013 Best Session Paper Award, 2010 Takayanagi Research Encourage Award, 2010 Paper Award of Japan Society of Technology Education, ICICIC2009 Best Paper Award, and ICINIS2009 Outstanding Contribution Award. He is a senior member of IEEJ and a member of IEICE, INASS, and JSTE.

Kanji Abe was born in Fukuoka, Japan in 1993. He received the B.Eng. degree from Fukuoka Institute of Technology, Fukuoka, Japan in 2014. His research interests switched-capacitor power supply. From 2014, he has been with Graduate School of Engineering, Fukuoka Institute of Technology, where he is now a first year master's student. Mr. Abe received ICIAE2015 Best Presentation Award.

Sawai Pongswatd was born in Bangkok, Thailand in 1971. He received the B.Eng., the M.Eng., and the D.Eng. degree from King Mongkut's Institute of Technology Ladkrabang, Bangkok, Thailand in 1994, 1997, and 2010, respectively. His research interests include programmable logic control, energy conversion, factory automation, and fieldbus technology. From 1995, he has been with King Mongkut's Institute of Technology Ladkrabang, where he is now an Associate Professor. Dr. Sawai received ICICIC2009 Best Paper Award.

Shinya Terada was born in Yamaguchi, Japan in 1979. He received the B.Eng., the M.Eng., and the D.Eng. degree from Sojo University, Kumamoto, Japan in 2002, 2005, and 2007, respectively. His research interests switched-capacitor power supply. From 2007, he has been with Kumamoto National College of Technology, where he is now an Associate Professor. Dr. Terada received Student Paper Award in IEEE MWSCAS 2004. He is a member of IEICE and IEEE.

Ichirou Oota was born in Miyazaki, Japan in 1955. He received the B.Eng., the M.Eng., and the D.Eng. degree from Kumamoto University, Kumamoto, Japan in 1979, 1981, and 1991, respectively. His research interests include switched capacitor circuits, switching converters, and computer simulation for switching circuits. From 1981, he has been with Kumamoto National College of Technology, where he is now a Professor. From 1994 to 1995, he was an oversea researcher in University of California, Berkeley. Prof. Dr. Oota is a member of IEICE and IEEJ.